Detection of high-energy adsorbate vibrational modes by atom-surface scattering

Yarong Tang and J. R. Manson
Department of Physics and Astronomy, Clemson University, Clemson, South Carolina 29634

K.-H. Rieder
Fachbereich Physik, Freie Universität Berlin, Arnimallee 14, D-14195 Berlin, Germany
(Received 8 March 2000; revised manuscript received 26 July 2000)

It is suggested that high-frequency vibrational modes of surface adsorbates can produce very characteristic signature features in the observable inelastic intensity in experiments using atomic beams as scattering probes. These features consist of peaks in the inelastic background, due to multiquantum excitation of the high-energy vibrational modes, and these peaks are significantly broadened and shifted in the direction of energy loss by the multiphonon scattering arising from the substrate and other low-energy adsorbate modes. Calculations for the scattering of rare gases from several types of adsorbate indicate that, by selecting the probe projectile species and tuning the incident energy and incident beam angle, selected high-energy modes can be excited, and the method can be used to accurately measure the vibrational frequencies and polarizations of these modes.

I. INTRODUCTION

The primary methods currently used for determination of vibrational frequencies at both clean and adsorbate-covered surfaces are electron energy-loss spectroscopy (EELS),[1] infrared spectroscopy (IR),[2] and He atom scattering.[3,4] Of these methods, He atom scattering has been particularly successful at measuring the dispersion curves and obtaining other surface dynamic information for many clean and adsorbate-covered surfaces at low energies, energies significantly less than 100 meV. For higher-energy adsorbate modes, those with energies typically less than 0.5 eV, EELS and IR are generally considered to be much more appropriate measurement techniques. More recently, energy-resolved scanning tunneling microscopy has been demonstrated capable of detecting high-frequency adsorbate modes,[5–7] and in some cases low-frequency modes.[6,7]

In this paper we wish to address the question of whether higher-energy adsorbate vibrational modes can be observed by atom-surface scattering, in particular by exploiting the higher energies and heavier projectile masses provided by monoenergetic and well-collimated free jet beams of the heavier rare gases. Generally, experiments on the scattering of the heavier rare gases exhibit far fewer quantum-mechanical features than He atom scattering, although significant diffraction and single-quantum phonon exchange have been observed with low-energy Ne scattering.[8,9] The scattered intensity observed in experiments with heavy rare gases and even Ne and He at higher energies usually consists of broad featureless lobes due to classical multiphonon scattering.[10–12] What we demonstrate here is that, under certain initial conditions, high-energy modes can give rise to characteristic signature peaks in this multiphonon inelastic background due to energy losses from single- and multiple-quantum excitation. These peaks are not sharp and well defined, as one might expect from an EELS or IR experiment, rather they are considerably broadened by multiphonon energy transfers with the low-frequency substrate modes and other low-frequency modes due to the adsorbates. However, with proper analysis of these high-energy features, it is shown that the frequencies of the high-energy adsorbate modes should be accurately measurable.

If one considers the atom-surface scattering problem from a purely quantum-mechanical viewpoint, then arguments based on the Debye-Waller factor would tend to predict that no quantum-mechanical features should be observable in the high-energy limit. All quantum features, such as elastic diffraction peaks and single-quantum phonon peaks, are multiplied by the Debye-Waller factor $\exp(-2W)$; in the simplest analysis the Debye-Waller argument is given by $2W=\langle(\mathbf{p}\cdot\mathbf{u})^2\rangle/\hbar^2$, where $\mathbf{p}=\mathbf{p}_f-\mathbf{p}_i$ is the scattering vector for a scattering transition from initial momentum $\mathbf{p}_i$ to final state $\mathbf{p}_f$ and $\mathbf{u}$ is the vibrational displacement vector of the surface. The physical interpretation of the value of $2W$ is that it is the average number of phonons exchanged in a scattering event. Thus in classical scattering, where $2W$ is large, the Debye-Waller factor is small and all quantum features are suppressed, and all that can be observed is a broad inelastic background due to the multiphonon exchange. However, what we show here is that, with appropriately chosen initial conditions, the single-quantum and sometimes the multiple-quantum excitations of high-energy adsorbate modes can be observed under conditions in which the Debye-Waller factor is negligibly small. In these cases the high-energy peaks appear as energy-loss (quantum creation) events and they are broadened by the multiple-quantum exchanges with the low-energy modes of the substrate. Nevertheless, they appear as very characteristic features and analysis and comparison of these peak shapes and positions with theoretical models such as those presented here should lead to methods for accurately determining the high-energy mode frequencies.

We present here two different models of the scattering process. Both models consider a surface adsorbate with a single high-frequency mode in the 0.25–0.5 eV range. The first of these models treats the multiphonon background arising from the substrate as the semiclassical or classical limit of scattering from a Debye solid. The other model uses the low-frequency modes of the adsorbate to simulate the inelas-

tic background of the substrate. The results of calculations for both models are qualitatively and quantitatively quite similar.

Our calculations indicate that by carefully choosing the species of the scattering projectile and by tuning the incident energy and incident angle the high-frequency modes can be selected and will have distinct characteristic features which can be used to determine the mode energies and provide information on the polarization.

This paper is organized in the following manner. In the next section the theory is developed and the two models used for calculations are presented. In Sec. III calculations are carried out for several different adsorbate species and for the rare gases He and Ne, as scattering projectiles. The conclusions that can be drawn from this work are discussed in Sec. IV.

II. THEORY

A. General treatment

An appropriate starting point for a general treatment of inelastic scattering between a projectile and a many-body target is the quantum-mechanical transition rate, or generalized Fermi golden rule, for the projectile to scatter from the initial state of momentum $\mathbf{p}_i$ to the final state $\mathbf{p}_f$, which is given by[13,14]

$$w(\mathbf{p}_f,\mathbf{p}_i)=\left\langle \frac{2\pi}{\hbar}\sum_{\{n_f\}} |\langle n_f,\mathbf{p}_f|\mathcal{T}|\mathbf{p}_i,n_i\rangle|^2\delta(\mathcal{E}_f-\mathcal{E}_i)\right\rangle, \quad (1)$$

where $|n_i\rangle$ is the initial many-body state of the unperturbed target, the $\Sigma_{\{n_f\}}$ is a summation over all final states of the target, $\mathcal{T}$ is the transition operator $\mathcal{E}_f$ and $\mathcal{E}_i$ are, respectively, the final and initial energy of the entire system of target plus projectile, and the angular brackets, $\langle\,\rangle$ signify an average over all initial target states. In atom-surface scattering the measured intensities are usually differential reflection coefficients, which are obtained from the transition rate upon multiplication by the density of final scattering states as follows:

$$\frac{dR}{d\Omega_f dE_f}=\frac{L^4}{(2\pi\hbar)^4}\frac{m^2|\mathbf{p}_f|}{p_{iz}}w(\mathbf{p}_f,\mathbf{p}_i), \quad (2)$$

where m is the mass of the projectile atom and p_{iz} is the component of the incident momentum perpendicular to the surface.

A quite general expression for the transition rate for the full transition operator can be obtained in the semiclassical limit. This involves making the approximations of assuming that the collision is fast in comparison to phonon periods, that it is sufficient to expand the interaction potential through terms linear in the atomic displacements, and that all the substrate atoms in the surface layer are identical. All of these approximations have been justified in detail in connection with development of multiphonon exchange in atom-surface scattering, and have been shown to be valid through extensive comparison with experimental measurements.[11,14–16] The result is the following form for the transition rate:

$$w(\mathbf{p}_f,\mathbf{p}_i)=\frac{1}{\hbar^2}|\tau_{fi}|^2e^{-2W(\mathbf{p})}\int_{-\infty}^{+\infty}dt\,e^{-i(E_f-E_i)t/\hbar}e^{Q(\mathbf{p},t)}. \quad (3)$$

In the semiclassical approximation of quick collisions, the time-dependent correlation function $Q(\mathbf{p},t)$ is given by the displacement correlation function

$$Q(\mathbf{p},t)=\frac{1}{\hbar^2}\langle\mathbf{p}\cdot\mathbf{u}(0)\mathbf{p}\cdot\mathbf{u}(t)\rangle, \quad (4)$$

where $\mathbf{p}=\mathbf{p}_f-\mathbf{p}_i$ and the argument of the Debye-Waller factor is $2W(\mathbf{p})=Q(\mathbf{p},t=0)$ as discussed above in Sec. I. In Eq. (3) the energies E_f and E_i are, respectively, the final and initial kinetic energies of the scattered projectile. The factor $|\tau_{fi}|^2$ is the form factor, which depends on the nature of the scattering center and the interaction potential. For all calculations carried out below in Sec. III we take $|\tau_{fi}|^2$ to be a constant, which has been shown to be appropriate for hard core scattering. The expression of Eq. (3) is well known, and is the basis for many dynamical scattering theories in quite different areas of physics.[17,18]

If the crystal target together with its adsorbates is a harmonic system, then the displacement $\mathbf{u}(t)$ can be decomposed into harmonic mode components. One can then arbitrarily divide $\mathbf{u}(t)$ into two sets $\mathbf{u}_1(t)$ and $\mathbf{u}_2(t)$ as $\mathbf{u}(t)=\mathbf{u}_1(t)+\mathbf{u}_2(t)$. If we now choose the set $\mathbf{u}_1(t)$ to contain only the normal-mode components of the low-frequency modes and place the high-frequency adsorbate mode(s) in $\mathbf{u}_2(t)$, then the two sets of modes remain orthogonal and the time-dependent correlation coefficient of Eq. (4) becomes the sum of two terms,

$$Q(\mathbf{p},t)=Q_1(\mathbf{p},t)+Q_2(\mathbf{p},t)=\frac{1}{\hbar^2}\langle\mathbf{p}\cdot\mathbf{u}_1(0)\mathbf{p}\cdot\mathbf{u}_1(t)\rangle + \frac{1}{\hbar^2}\langle\mathbf{p}\cdot\mathbf{u}_2(0)\mathbf{p}\cdot\mathbf{u}_2(t)\rangle. \quad (5)$$

When Eq. (5) is used with Eq. (3) the transition rate takes a form which is the starting point for further calculations:

$$w(\mathbf{p}_f,\mathbf{p}_i)=\frac{1}{\hbar^2}|\tau_{fi}|^2e^{-2W_1(\mathbf{p})}e^{-2W_2(\mathbf{p})} \times\int_{-\infty}^{+\infty}dt\,e^{-i(E_f-E_i)t/\hbar}e^{Q_1(\mathbf{p},t)}e^{Q_2(\mathbf{p},t)}. \quad (6)$$

This is the Fourier convolution of two independent exponentiated time-dependent correlation functions. Writing the integrand of Eq. (6) as the product of two exponential functions requires that the reduced correlation functions $Q_1(\mathbf{p},t)$ and $Q_2(\mathbf{p},t)$ commute with each other. In general, since the two functions usually involve orthogonal harmonic modes they will automatically commute, but for the purposes of this work we will take the substrate correlation function $Q_1(\mathbf{p},t)$ in the classical limit; thus in this limit commutation is always assured.

B. High-frequency mode

The first step in developing model calculations is to consider the problem of a single Einstein mode oscillator on an otherwise rigid substrate. This is obtained upon setting $Q_1(\mathbf{p},t)=0$ and evaluating $Q_2(\mathbf{p},t)$ for a single harmonic mode of frequency Ω. This is a well-known problem and the result is[19,20]

$$w(\mathbf{p}_f,\mathbf{p}_i)=\frac{2\pi}{\hbar}|\tau_{fi}|^2 e^{-2W(\mathbf{p})} \times\sum_{\alpha=-\infty}^{\infty} I_{|\alpha|}\left(\frac{\mathbf{P}^2}{\hbar\Omega M_\Omega}\sqrt{n(\Omega)[n(\Omega)+1]}\right) \times\left(\frac{n(\Omega)+1}{n(\Omega)}\right)^{\alpha/2}\delta(E_f-E_i+\alpha\hbar\Omega), \tag{7}$$

where M_Ω is the oscillator effective mass, which can be determined from a normal-mode analysis, $\mathbf{P}$ is the component of $\mathbf{p}$ parallel to the Cartesian direction of the oscillator motion, $n(\Omega)$ is the Bose-Einstein function, k_B is the Boltzmann constant, and $I_\alpha(z)$ is the modified Bessel function of integral order α and argument z. The argument of the Debye-Waller factor is given by $W(\mathbf{P})=\mathbf{P}^2[n(\Omega)+\frac{1}{2}]/2\hbar\Omega M_\Omega$.

The analysis leading up to Eq. (7) shows that the exponentiated dynamical correlation function of a single Einstein oscillator can be Fourier decomposed into the following series:

$$e^{Q_2(\mathbf{p},t)}=\sum_{\alpha=-\infty}^{\infty} e^{-i\alpha\hbar\Omega t/\hbar} I_{|\alpha|} \times\left(\frac{\mathbf{p}^2}{\hbar\Omega M_\Omega}\sqrt{n(\Omega)[n(\Omega)+1]}\right)\left(\frac{n(\Omega)+1}{n(\Omega)}\right)^{\alpha/2}. \tag{8}$$

C. Substrate modeled by a Debye model

A simple model for describing the vibrational energy exchanges with a surface substrate in the classical and semiclassical limit, one that has the additional advantage of producing an analytic closed-form expression for the differential reflection coefficient, is to assume that the surface is a collection of discrete scattering centers each of which is vibrating with a bulk Debye frequency spectrum. The transition rate for such a model, in the absence of adsorbate modes, is the well-known expression[14,21–23]

$$w(\mathbf{p}_f,\mathbf{p}_i)=\frac{2\pi}{\hbar}|\tau_{fi}|^2\frac{1}{\sqrt{4\pi Z(T_S)\Delta E_0}} \times\exp\left\{-\frac{(E_f-E_i+\Delta E_0)^2}{4Z(T_S)\Delta E_0}\right\}, \tag{9}$$

where T_S is the surface temperature, $\Delta E_0=\mathbf{p}^2/2M_C$ is the recoil energy of the collision with the substrate atom of mass M_C and the temperature-dependent function $Z(T_S)$ is given by

$$Z(T_S)=3k_B\Theta_D\int_0^1 d\omega\,\omega^3\left(\frac{1}{\exp(\Theta_D\omega/T_S)-1}+\frac{1}{2}\right), \tag{10}$$

where Θ_D is the Debye temperature. At surface temperatures large compared with the Debye temperature $Z(T_S)$ has the limiting form $Z(T_S)\to k_BT_S$. Note that in this high-temperature limit the transition rate of Eq. (9) becomes independent of the Debye temperature, and indeed, becomes a model-independent function of the mass M_C and temperature T_S with no free adjustable parameters.

Equation (9) is a semiclassical model whose physical interpretation is quite straightforward. The scattering is governed by three principal factors: (1) the form factor $|\tau_{fi}|^2$ is determined from the nature of the scattering center; (2) the envelope factor $1/\sqrt{4\pi Z(T_S)\Delta E_0}$ shows that the maximum value of the peak decreases with the square root of the surface temperature and with the square root of ΔE_0; and (3) the peak shape is dictated by the Gaussian-like function in the energy transfer E_f-E_i. This peak, however, is not a true Gaussian. Instead, it is skewed at both high and low energies because of the energy dependence of the recoil energy loss ΔE_0. For example, at high temperatures but low incident energies, the peak becomes very nearly exponential in form.[16] The width of the peak, under conditions in which it does appear Gaussian-like, increases at large temperatures as the square root of the temperature and the square root of ΔE_0.

In spite of its simplicity, this model when used with a constant form factor has been quite useful in describing the multiphonon backgrounds measured in numerous atom-surface experimental configurations for many different substrates and a range of scattering projectiles,[16,24,25] as well as for other systems such as neutron scattering.[21] The constant form factor, which describes hard-core scattering from spherical segments of the target, has been demonstrated to be appropriate for atom-surface scattering at energies in the range considered here.[24,25] For these reasons, this appears to be an ideal model to illustrate the multiquantum contributions of the substrate to the problem at hand.

It is also interesting to note that the the treatment leading to the transition rate of Eq. (9) gives, as an intermediate step, the exponentiated dynamical correlation factor $e^{Q_1(\mathbf{p},t)}$ in the following form:

$$e^{Q_1(\mathbf{p},t)}=e^{-i\Delta E_0 t/\hbar}e^{-\Delta E_0 Z(T_S)t^2/\hbar^2}. \tag{11}$$

We are now in a position to determine the full expression for a system with the single high-frequency mode of Sec. II B adsorbed on a substrate modeled by the Debye system of this section. This is accomplished by using, for the two exponentiated dynamical correlation functions in the full expression for the transition rate of Eq. (6), Eq. (8) for $Q_2(\mathbf{p},t)$ of the high-frequency mode and Eq. (11) for the $Q_1(\mathbf{p},t)$ of the substrate modes. The Fourier convolution is straightforward and the result is

$$w(\mathbf{p}_f,\mathbf{p}_i)=\frac{1}{\hbar}|\tau_{fi}|^2\sqrt{\frac{\pi}{Z(T_S)\Delta E_0}}e^{-2W(\mathbf{P})}\times\sum_{\alpha=-\infty}^{\infty}I_{|\alpha|}\left(\frac{\mathbf{P}^2}{\hbar\Omega M_\Omega}\sqrt{n(\Omega)[n(\Omega)+1]}\right)\times\left(\frac{n(\Omega)+1}{n(\Omega)}\right)^{\alpha/2}\times\exp\left\{-\frac{(E_f-E_i+\Delta E_0+\alpha\hbar\Omega)^2}{4Z(T_S)\Delta E_0}\right\}. \quad (12)$$

Equation (12) is seen to be a series of Gaussian-like peaks, similar in form to Eq. (9), each being centered at an energy loss or gain given by the multiquantum excitations of the high-frequency mode Ω. The relative heights of these peaks are governed by the strength of the corresponding high-frequency multiquantum overtones. It is clear that in the case of scattering at temperatures in the region of room temperature or less, the Bose-Einstein factor $n(\Omega)$ will be essentially zero for large Ω and these features will appear only for energy-loss (phonon creation) transfers.

The physical nature of these broadened Gaussian-like peaks is clear. Instead of observing sharp peaks due to the zero-, single-, and multiple-quantum losses at roughly the final energy values $E_f=E_i-\alpha\hbar\Omega$, these sharp peaks are broadened by multiphonon exchange with the low-energy surface modes. Each of these broadened peaks appears as an individual multiquantum peak similar to the typical single broad multiquantum peak that is observed from clean, close-packed surfaces under semiclassical scattering conditions, but the center of each of these peaks is shifted in the direction of energy loss according to the effect of the recoil energy transfer ΔE_0 as it appears in Eq. (12).

Equation (12) is for a full coverage layer of adsorbates, for which the substrate is completely covered. In the case of a partial layer coverage where a fraction of the projectiles scatter from bare regions of the substrate the contribution of Eq. (12) will be reduced proportionately, and there will be additional multiphonon scattering in the neighborhood of the $\alpha=0$ peak of Eq. (12) arising from scattering from the bare substrate. Equation (12) constitutes the Debye model that we use in Sec. III to illustrate the effect of the substrate modes on the high-frequency quantum energy-loss peaks.

D. Low-frequency modes modeled by an Einstein oscillator

Next, we treat the low-frequency mode contribution from the substrate as a single low-frequency Einstein oscillator. It will become apparent that in the classical limit one oscillator is sufficient, and no new qualitative or quantitative contributions appear if several, or even a distribution of, Einstein oscillators are utilized.

In this case the dynamical correlation function for the high-energy mode of frequency Ω is again given by Eq. (8). For the low-energy mode, whose frequency will be denoted by ω, the correlation function is given by a similar expression with Ω replaced by ω, $\mathbf{P}$ replaced by $\mathbf{P}_1$, and M_Ω replaced by M_1, the effective mass of the substrate oscillators. $\mathbf{P}_1$ is the Cartesian component of the momentum transfer vector $\mathbf{p}$ in the direction of motion of the low-frequency oscillator, and for simplicity in the remainder of this work we will assume that this is the direction normal to the surface, in which case $P_1=|k_{fz}|+|k_{iz}|$, i.e. this corresponds to the case of the Einstein mode associated with vertical motion of a single layer of adsorbed atoms on the surface.

When these correlation functions are used in Eq. (6) the result is a transition rate of the following form:

$$w(\mathbf{p}_f,\mathbf{p}_i)=\frac{2\pi}{\hbar}|\tau_{fi}|^2e^{-2W_1(\mathbf{P}_1)}e^{-2W(\mathbf{P})}\times\sum_{\alpha=-\infty}^{\infty}I_{|\alpha|}\left(\frac{\mathbf{P}^2}{\hbar\Omega M_\Omega}\sqrt{n(\Omega)[n(\Omega)+1]}\right)\times\left(\frac{n(\Omega)+1}{n(\Omega)}\right)^{\alpha/2}\times\sum_{\beta=-\infty}^{\infty}I_{|\beta|}\left(\frac{\mathbf{P}_1^2}{\hbar\omega M_1}\sqrt{n(\omega)[n(\omega)+1]}\right)\times\left(\frac{n(\omega)+1}{n(\omega)}\right)^{\beta/2}\delta(E_f-E_i+\alpha\hbar\Omega+\beta\hbar\omega). \quad (13)$$

As discussed above in Sec. II A, Eq. (13) is to be considered only when the energy transfers due to the small frequency ω are taken in the classical limit, which implies large numbers of exchanged quanta. The argument of the Debye-Waller factor provides an estimate of the average number of exchanged quanta in a given scattering event, so the application of Eq. (13) depends on $W_1(\mathbf{P}_1)$ being large. Under these conditions, the spectrum produced by the transition rate of Eq. (13) consists of densely packed δ-function peaks whose amplitudes lie under a smoothly varying envelope function. In the classical limit the δ-function peaks are so dense that they cannot be experimentally resolved, and what is observed is the integrated intensity or the envelope function. This is the limit in which Eq. (13) is strictly valid and the limit in which we will use in this work.

III. MODEL CALCULATIONS

A. He atom scattering from the CO stretch mode

In this section we calculate a series of different adsorbate configurations in an attempt to demonstrate that high-frequency modes should be observable in atom-surface scattering. As the first step in this process it is of interest to illustrate the system considered above in Sec. II D in which the substrate modes are modeled by a single low-frequency mode.

Figure 1 shows calculations for He atom scattering at an incident energy $E_i=1$ eV in which the high-frequency mode is chosen to be the carbon monoxide C-O stretch mode when the CO is adsorbed on a Cu(001) surface. In this case, $\hbar\Omega=257.8$ meV and the effective mass of the oxygen atom as calculated from a simple two-spring/two-mass model for CO on a rigid surface is $M_\Omega=30.80$ amu.

The substrate mass is chosen to be $M_1=132.29$, which corresponds to the Einstein mode observed for a single monolayer of xenon on Cu(001) having an energy $\hbar\omega$

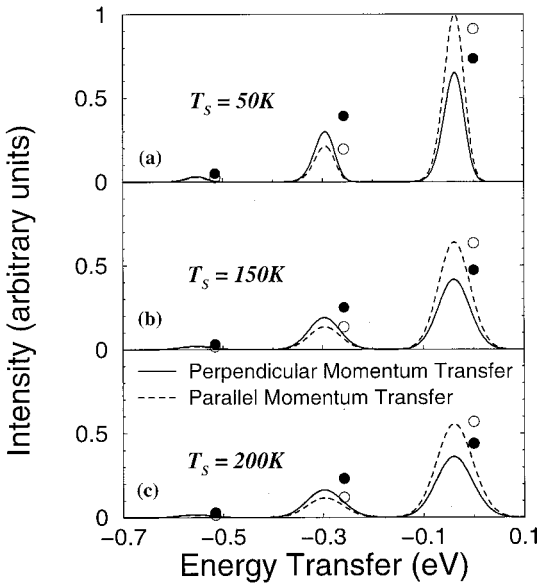

FIG. 1. The scattered intensity versus energy transfer $E_f - E_i$ for a 1 eV, incident beam of He atoms scattering from the C-O stretch mode of CO adsorbed on Cu(001). The substrate phonons are modeled by a single low-frequency Einstein mode. The incident and final polar angles are $\theta_i = 78°$ and $\theta_f = 18°$ and the surface temperatures are $T_S =$ (a) 50, (b) 150, and (c) 200 K. The solid curve shows the calculation for the CO in its actual vertical on-top configuration, while the dashed curve shows the results of the calculation if one arbitrarily assumes that the CO is lying flat with the C-O bond parallel to the surface. The points marked by large circles at multiples of $\hbar\Omega = 258$ meV are the positions and relative intensities of the CO stretch-mode overtone energy-loss peaks if the substrate were rigid, with filled circles denoting the vertical on-top CO configuration and open circles denoting the flat-lying CO configuration.

$= 2.71$ meV.[26] The surface temperature is $T_S = 50$ K for Fig. 1(a), 150 K for Fig. 1(b), and 200 K for Fig. 1(c). The incident beam polar angle is $\theta_i = 78°$ with respect to the surface normal, and the detector angle is $\theta_f = 18°$ with the incident and final directions in the same plane as the surface normal (i.e., scattering in the sagittal plane). This geometry corresponds to an angle between the incident beam and detector directions of $\theta_{SD} = \theta_i + \theta_f = 96°$, which is typical of many experiments.

Although Eq. (13) consists of a series of equally spaced sharp δ-function peaks, the calculated curves shown in Fig. 1 are the envelope functions of these densely packed peaks. The large circles show the relative positions and intensities that the high-frequency oscillator energy-loss overtones would exhibit if there were no low-energy multiquantum energy exchange, i.e., if the substrate were rigid. In order to test the fact that the envelope function is independent of the substrate phonon energy several calculations were carried out for a succession of values of the low frequency ω. The envelope function showed essentially no change for values of $\hbar\omega < 10$ meV, which corresponds to roughly 5% of the CO stretch energy $\hbar\Omega$. The calculations in Fig. 1 were carried out with $\hbar\omega = 8$ meV.

The envelope function at all surface temperatures consists of two broad peaks of deceasing intensity and a much smaller third peak, each associated with one of the three high-frequency quantum overtones that have non-negligible

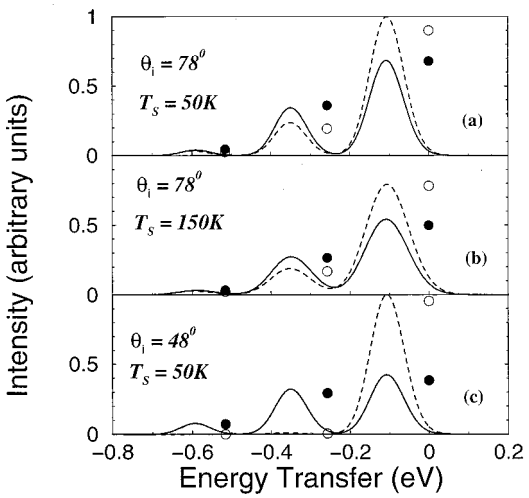

FIG. 2. (a), (b) Same as Figs. 1(a) and 1(b) except that the substrate phonons are calculated with a Debye model. (c) Same as (a) except for $\theta_i = \theta_f = 48°$.

intensity. These two broad peaks are redshifted to the energy-loss side of the corresponding high-frequency energy-loss positions. The fact that there are two distinct peaks, corresponding to the the zero- and single-quantum overtone energy-loss positions of the high-frequency mode, indicates that these high-frequency modes are indeed observable in spite of the fact that the energy transfers with the substrate modes are classical, i.e., in spite of the fact that the total Debye-Waller factor is negligibly small. Clearly the envelope function is essentially identical regardless of the value chosen for the low-frequency mode. This implies that the choice of low-frequency mode energy is not important just so long as it is much smaller than the high-frequency mode. Furthermore, it makes no essential difference if one uses one Einstein mode, or a distribution of several modes; the envelope will be identical in all cases as long as the low-energy modes are small compared to the high frequency.

The calculations shown in panels (a) and (b) of Fig. 2 are similar to those of Figs. 1(a) and 1(b) except the substrate modes are given by a Debye phonon model. The major difference with respect to the Einstein mode model of the substrate phonons of Fig. 1 is that the peaks are broader and the peak maxima are shifted to a larger value of energy loss with respect to the unperturbed C-O stretch overtone modes. This points out the fact that widely different substrate mode distributions can produce a quantitative difference in the observed scattering distribution, but not a qualitative difference.

Shown in Fig. 2(c) is a calculation that is the same as in (a) except with the incident and final angles now at $\theta_i = \theta_f = 48°$, i.e., at specular conditions. For the CO orientation perpendicular to the substrate, the results are quite similar to those of Fig. 1, except that there are now three broad peaks in the scattered spectrum. However, for the case of CO oriented parallel to the substrate there is only one broad peak, and the peaks resulting from the overtones of the O-O stretch mode are negligible. The reason for this is clear from Eq. (7) or Eq. (13) because the coupling to the CO mode is through the momentum exchange in the direction of the mode vibration. The vertically oriented CO couples to the perpendicular

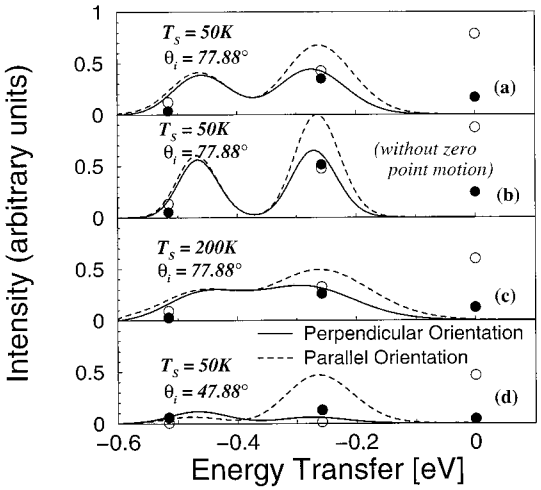

FIG. 3. The scattered intensity calculated for Ne atoms with $E_i = 0.6$ eV incident on CO adsorbed on Cu(001). The solid curve is for CO oriented vertically, while the dashed curve is for the hypothetical case of CO oriented horizontally on the surface. (a) $\theta_i = 78°$, $\theta_f = 18°$, and $T_S = 50$ K; (b) same as (a) except calculated without the effects of quantum-mechanical zero-point motion; (c) same as (a) except for the higher surface temperature $T_S = 200$ K; and (d) same as (a) except now for the specular conditions $\theta_i = \theta_f = 48°$.

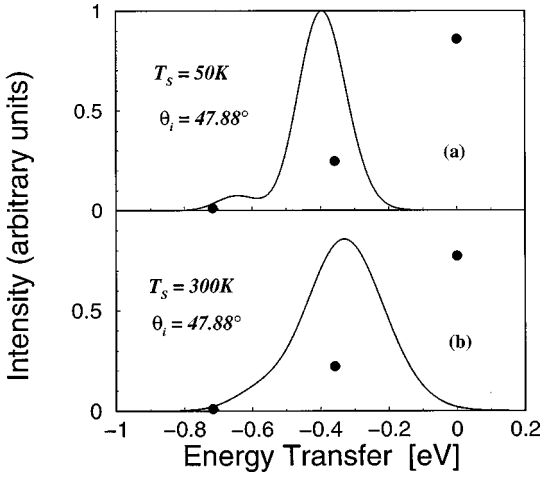

FIG. 4. The scattered intensity versus energy transfer $E_f - E_i$ for a model of a 1 eV incident beam of Ne atoms scattering from the C-H stretch mode of C_2H_2 adsorbed on Cu(001) with $\hbar\Omega = 358$ meV. Only the C-H stretch mode is included in the model of the C_2H_2 adsorbate. The substrate phonons are modeled by a Debye solid. The C-H stretch bond is oriented horizontally on the surface. (a) $\theta_i = \theta_f = 48°$ and $T_S = 50$ K; (b) same as (a) except for the higher surface temperature $T_S = 300$ K.

momentum exchange $p_z = |p_{fz}| + |p_{iz}|$ which, for a ''fixed angle'' experimental apparatus with $\theta_i + \theta_f$ constant, does not change substantially with the incident angle. However, the parallel-oriented CO couples to the parallel momentum exchange $\mathbf{P} = \mathbf{P}_f - \mathbf{P}_i$, which is quite small near specular conditions but large at grazing incident or final angles. The results of Fig. 2(c) make it clear that the experiment can be tuned to select modes of a particular orientation by properly choosing the incident and final scattering angles in order to maximize the momentum transfer in the direction of the vibrational displacement of the mode, i.e., such measurements should be sensitive to the polarization of the adsorbate modes.

B. Ne atom scattering from the CO stretch mode

Figure 3 shows a series of calculations for the scattering of Ne atoms with an incident energy $E_i = 0.6$ eV from a substrate with CO adsorbates, again with the substrate modes taken as a Debye model. Figure 3(a) is for $\theta_i = 78°$, $\theta_f = 18°$, and a surface temperature $T_S = 50$ K. The solid curve shows the results for CO oriented vertically on the surface and the dashed curve is for the hypothetical case of CO oriented horizontally on the surface. As above in the case of He scattering from this same system, there are two distinct but broadened peaks, one arising from the zero-quantum excitation of the C-O stretch mode, and the other arising from the single-quantum energy-loss C-O excitation.

Figure 3(b) shows the same system as in Fig. 3(a) except that the calculation is done without including the effects of zero-point motion in the substrate modes. The neglect of zero-point motion is easily effected in the calculation by replacing $Z(T_S)$ in Eq. (13) by its high-temperature limit $k_B T_S$. This calculation points out clearly that the effects of zero-point motion are important and should be quite measurable even for a projectile as heavy as Ne. The two peaks are significantly narrower than in the correct quantum-mechanical calculation of Fig. 3(a), although the energy shifts in the two calculations are approximately the same.

Figure 3(c) presents a calculation that is the same as in Fig. 3(a) except that the substrate temperature is now taken to be $T_S = 200$ K. The presence of the single-quantum overtone of the C-O stretch mode is still evident as a shoulder at approximately the same energy loss as in Fig. 3(a). The effect of higher temperatures is quite strong with this heavier projectile and it is clear that distinct peaks will form only at low temperatures where zero-point motion has an important effect.

Figure 3(d) shows a calculation that is the same as in Fig. 3(a) except carried out at the specular condition in which $\theta_i = \theta_f = 48°$. Again, as in Fig. 2(c), this shows that changing the incident and final scattering angles can make a big difference in the scattering distribution. In the case of vertical CO orientation, the slightly larger value of normal momentum transfer increases the relative importance of the single-quantum C-O stretch overtone so that two nearly equal peaks appear. For the case of horizontally oriented CO the single-quantum overtone contribution is visible as a smaller peak, whereas in Fig. 2(c) it is seen that for He scattering under nearly the same conditions this contribution is completely negligible.

C. Ne atom scattering from the C-H stretch mode

As a final example of the possibility of measuring high-frequency surface modes with atom scattering, Fig. 4 shows calculations of Ne incident with $E_i = 1$ eV losing energy to the C-H bond mode of a typical organic molecule. In this case, the energy of the mode corresponds to that of acetylene C_2H_2, adsorbed on Cu(001), which is $\hbar\Omega = 358$ meV.[27] The

C-H bond lies parallel to the surface and thus interacts only with the parallel momentum exchange. Figures 4(a) and 4(b) show the results for near-specular incidence conditions with $\theta_i = \theta_f = 48°$. At low temperatures, panel (a) shows that there are two distinct peak features in the multiphonon spectrum; however, the redshift of these features is as large as or larger than the 0.4 eV energy of the C-H mode itself. Panel (b) calculated with $T_S = 300\,\mathrm{K}$ shows that there is considerable thermal smearing at high temperatures; thus such experiments will be effective only if carried out at very low temperatures.

IV. CONCLUSIONS

We have investigated the possibility of using atomic beam scattering at hyperthermal energies to make observations of high-frequency surface adsorbate modes. In general, when scattering heavy-mass and high-energy atoms from surfaces, classical scattering conditions prevail and what is seen is smooth angular lobes, and when these angular lobes are energy analyzed the energy-resolved spectra also exhibit smooth broad peaks. However, when the incident atomic translational energy is larger than but comparable to that of a high-energy adsorbate frequency mode, such a mode may be excited with low quantum excitation numbers, e.g., single or double excitations. This can give rise to multiple peaks in the otherwise multiquantum energy-resolved scattering spectrum and, by properly tuning the incident beam energy and the orientation of the incident beam and detector, these distinguishable peaks can be used to identify the mode and evaluate its frequency.

In order to illustrate the possibilities of this process we have carried out calculations for the rare gases He and Ne scattering from several different adsorbate species. Two seemingly different models of the low-energy substrate modes have been tested, a Debye model and a model in which the substrate modes are taken to be a single low-frequency Einstein mode. The essential results for the two models are qualitatively quite similar, and are not substantially different in their quantitative aspects. Physically, this is easily understood because the extreme multiphonon limit is essentially classical scattering, and if the incident projectile energy is not large enough to actually penetrate the surface of the solid, then classical scattering is well represented by the impulsive collision limit, which does not depend on the details of the phonon spectrum.

The characteristic signature of the excitation of high-frequency adsorbate modes on the surface are distinct peaks in the diffuse inelastic background of the energy-resolved intensity spectra. These peaks are due to the single-, double-, and other low-quantum-number excitations of the high-frequency mode and they are broadened by the simultaneous excitation of large numbers of low-frequency substrate modes. The peaks are redshifted to lower energies due to the predominantly energy-loss excitations of the multiple quanta of low-frequency modes, and they appear separated in energy by somewhat less than the energy of the high-frequency adsorbate mode. Thus the energy of the high-frequency modes cannot be accurately determined from the actual positions of their characteristic peaks in the energy-resolved spectra, but by comparison with reasonably simple theoretical predictions such as those developed here, it should be possible to extract accurate values of their energies.

By choice of scattering projectile and by varying the incident energy and beam orientation, one can ''tune'' the experiment in order to enhance the signature peaks produced by particular adsorbate species. In particular, modes whose characteristic displacement is primarily perpendicular to the surface are most readily excited by experimental configurations that enhance the total momentum transfer of the projectile perpendicular to the surface. Modes that have vibrational displacements primarily parallel to the surface are best excited by maximizing the parallel momentum transfer. Thus it appears that such experiments should be able to distinguish the polarizations of the high-frequency adsorbate modes.

It is noteworthy that the theory presented here, when used with a constant form factor, has no freely adjustable parameters with the sole exception of the Debye temperature. However, the results for the Debye model are only very weakly dependent on the Debye frequency because it is used in the multiphonon limit.

The effect of surface temperature is rather dramatic and thermal smearing can easily mask the signature peaks; thus it will be best to reduce the temperature to the lowest possible value in order to reduce the multiphonon excitations of the low-frequency substrate modes.

This work provides an interesting example of the simultaneous coexistence of classical and quantum features. In the scattering regime considered here, the excitation number of the quantum creations of the high-frequency modes is small, implying that only a quantum-mechanical theory can be used. However, simultaneously extremely large numbers of low-frequency substrate modes are also excited. These excitation numbers are so large that the low-frequency excitations can be quite well approximated by classical or semiclassical calculations, in agreement with the correspondence principle, which in its simplest application implies that the regime of large-quantum-number excitations can be described by classical physics.

He atom scattering has already given abundant evidence of its unique ability to measure surface mode frequencies and related surface properties in the purely quantum limit in which the adsorbate energies and the incident He atom energies are very low, of the order of up to a few tens of meV. Here we show that, by increasing the incident energy and possibly by choosing a heavier rare gas atom as the projectile, much higher-energy adsorbate modes might be measured, such as those arising from chemisorption bonds.

ACKNOWLEDGMENTS

One of us (J.R.M.) would like to express appreciation to the Department of Physics of the Freie Universität Berlin for hospitality during part of this work. This work was supported by the U.S. Department of Energy under Grant No. DE-FG02-98ER45704, by the National Science Foundation under Grant No. DMR-9726229, and by the Deutsche Forschungsgemeinschaft, Sonderforschungsbereich 290 (TP A5).

[1] H. Ibach and D. L. Mills, *Electron Energy Loss Spectroscopy and Surface Vibrations* (Academic, New York, 1982).
[2] Andrew Zangwill, *Physics at Surfaces* (Cambridge University Press, Cambridge, 1988), p. 240.
[3] Daniel Farías and Karl-Heinz Rieder, Rep. Prog. Phys. **61**, 1575 (1998).
[4] *Helium Atom Scattering from Surfaces*, Vol. 27 of *Springer Series in Surface Sciences*, edited by E. Hulpke (Springer, Berlin, 1992).
[5] B. C. Stipe, M. A. Rezaei, and W. Ho, Science **289**, 1732 (1998).
[6] B. G. Briner (unpublished).
[7] F. Moresco, G. Meyer, and K.-H. Rieder, Mod. Phys. Lett. B **13**, 709 (1999).
[8] B. Salanon, J. Phys. (France) **45**, 1373 (1984); E. Semerad, P. Sequard-Base, and E. M. Hörl, Surf. Sci. **189/190**, 975 (1987).
[9] K.-H. Rieder and W. Stocker, Phys. Rev. Lett. **52**, 352 (1984).
[10] Kim Bolton, Marcus Svanberg, and Jan B. C. Pettersson, J. Chem. Phys. **110**, 5380 (1999); Mats B. Nȧgȧrd, Patrik U. Andersson, Nikola Marković, and Jan B. C. Pettersson, *ibid.* **109**, 10 339 (1998); E. K. Schweizer, C. T. Rettner, and S. Holloway, Surf. Sci. **249**, 335 (1991); Jean-Pierre Berthier, Alain Constans, Gérard Daury, and Pierre Lostis, C. R. Seances Acad. Sci., Ser. B **278**, 1067 (1974).
[11] M. F. Bertino, W. Silvestri, and J. R. Manson, J. Chem. Phys. **108**, 10 239 (1998).
[12] K.-H. Rieder and W. Stocker, Phys. Rev. B **31**, 3392 (1985).
[13] Leonard S. Rodberg and Roy M. Thaler, *Introduction to the Quantum Theory of Scattering* (Academic, New York, 1967), Chap. 8.
[14] J. R. Manson, Phys. Rev. B **43**, 6924 (1991).
[15] R. Brako and D. M. Newns, Phys. Rev. Lett. **48**, 1859 (1982); Surf. Sci. **123**, 439 (1982).
[16] J. R. Manson, Comput. Phys. Commun. **80**, 53 (1994).
[17] C. Kittel, *Quantum Theory of Solids* (Wiley, New York, 1963), Chap. 19.
[18] A. A. Maradudin, E. W. Montroll, and G. H. Weiss, *Theory of Lattice Dynamics in the Harmonic Approximation*, Suppl. 3 in *Solid State Physics*, edited by F. Seitz and D. Turnbull (Academic, New York, 1963), Chap. VII.
[19] J. R. Manson, Phys. Rev. B **37**, 6750 (1988).
[20] Gerald D. Mahan, *Many-Particle Physics* (Plenum, New York, 1990), p. 293.
[21] A. Sjölander, Ark. Fys. **14**, 315 (1959).
[22] J. R. Manson, J. Phys.: Condens. Matter **5**, A283 (1993).
[23] D. A. Micha, J. Chem. Phys. **74**, 2054 (1981).
[24] A. Muis and J. R. Manson, J. Chem. Phys. **107**, 1655 (1997).
[25] A. Muis and J. R. Manson, J. Chem. Phys. **111**, 730 (1999).
[26] B. Gumhalter, A. Šiber, and J. P. Toennies, Phys. Rev. Lett. **83**, 1375 (1999); A. Šiber, B. Gumhalter, J. Braun, A. P. Graham, M. F. Bertino, J. P. Toennies, D. Fuhrmann, and Ch. Wöll, Phys. Rev. B **59**, 5898 (1999); J. Braun, D. Fuhrmann, M. Bertino, A. P. Graham, J. P. Toennies, Ch. Wöll, A. Bilic, and B. Gumhalter, J. Chem. Phys. **106**, 9922 (1997).
[27] B. C. Stipe, M. A. Rezaei, and W. Ho, Phys. Rev. Lett. **82**, 1724 (1999).